Hardware implementation of PCM-based neurons with self-regulating threshold for homeostatic scaling in unsupervised learning

I. Muñoz-Martín*[+1], S. Bianchi[+1], S. Hashemkhani[1], G. Pedretti[1], and D. Ielmini[1]
[1]Dipartimento di Elettronica, Informazione e Bioingegneria (DEIB), Politecnico di Milano and IU.NET,
Piazza L. da Vinci 32, 20133, Milan, Italy, [+]Authors contributed equally, *email: irene.munoz@polimi.it

***Abstract*—Brain-inspired neuromorphic engineering aims at designing networks capable of learning from their own experience, in terms of both plasticity and stability. In biology, homeostatic scaling can regulate the frequency of neural processing in the brain and enable efficient synaptic learning activity. Implementing homeostatic regulation into hardware neural networks can thus enable stable, energy-efficient learning. Here, we present a novel artificial neuron based on phase change memory (PCM) devices capable of homeostatic regulation and power saving via self-adaptive threshold control. We experimentally show that this mechanism optimizes multi-pattern learning of the Fashion-MNIST dataset with asynchronous spike-timing-dependent plasticity (STDP). The PCM-based adaptive threshold is shown to act as a spike-frequency modulator of the whole neural network, giving robustness to the system against external perturbations. This work highlights the suitability of PCM devices for the optimization of synaptic dynamics and the implementation of brain-inspired neuromorphic circuits for cognitive agents and edge computing.**

***Keywords*—Unsupervised learning, spike-timing-dependent plasticity (STDP), homeostasis, spike-frequency adaptation, adaptive threshold, phase change memory (PCM).**

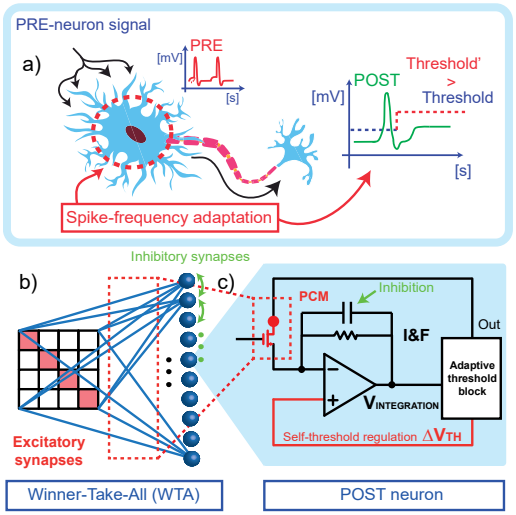

Fig. 1. Biological neurons collect input spikes (PRE) via the synaptic connections and modulate their response in frequency as a function of the spiking activity (a). This adaptive mechanism can be implemented into artificial neural networks, like unsupervised WTA via STDP, relying on a PCM device inside each neuron (b).

I. Introduction

In the last few years, the field of artificial intelligence (AI) has shown rapid progress, demonstrating high efficiency in tasks like image recognition, natural language processing and playing games [1-4]. Most of the AI systems rely on deep learning algorithms, where computational models achieve remarkable accuracy after the training of multiple layers with increasing level of abstraction [5]. However, to achieve good accuracy, AI systems need thousands or even millions of parameters that must be precisely tuned via time/energy expensive training algorithms [5]. On the other hand, the pre-tuning of the parameters deprives the systems of the necessary resilience for adaptation to a constantly changing environment, making this type of AI systems too rigid for real-life problems [6].

In biology, living organisms regulate their knowledge by plasticity-dependent mechanisms [7, 8], where the strength of the synaptic connection changes in response to the neural activity [9]. In particular, learning is usually enabled by Hebbian-type plasticity, where the time correlation between the pre-synaptic and post-synaptic spikes induces variations of the synaptic weights [10, 11]. An example of Hebbian-type learning is spike-timing-dependent plasticity (STDP) [12]. The drawbacks of Hebbian learning, however, are the excessive synaptic potentiation and spiking activity due to the positive correlation between the response of the neuron and its inputs [13]. To avoid these issues, biological systems adopt homeostatic regulation, where the neuron maintains a stable spiking activity to prevent saturation of the synaptic elements. Homeostatic regulation thus allows to stabilize the neural spiking activity in response to an unwanted change of the firing rate due to an external perturbation [9]. In particular, homeostatic scaling, also known as synaptic scaling [14], refers to a decrease of the synaptic strength to counteract a chronically elevated firing rate of a population of neurons. Hebbian learning and homeostatic regulation thus cooperate to optimize experience-driven knowledge to achieve lifelong processing, adaptation and stability of real-life information [15, 16].

Brain-inspired electronic systems usually rely on spiking neural networks (SNNs) for emulating biological cognitive functions like synaptic dynamics in unsupervised learning. Various neuromorphic SNNs based on CMOS technology have been proposed in literature, demonstrating the possibility of building VLSI synaptic circuits with homeostatic neurons [17-19]. At the same time, memory devices, such as resistive-random-access memory (RRAM) and phase change memory (PCM), have emerged as promising synaptic elements for neuromorphic computation, thanks to reduced area, 3D stacking capability and analog storage [20, 21]. In particular, PCMs have recently demonstrated outstanding multi-level capability [22], rising as efficient synaptic elements to enable continual learning in neural networks [23, 24].

This work presents a new neuronal structure with a self-regulating threshold for spike-frequency adaptation at

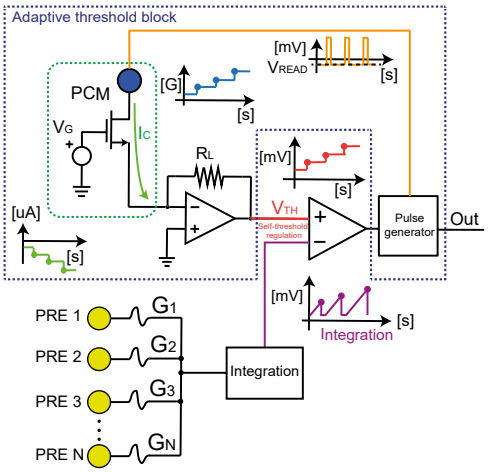

Fig. 2. Schematic representation of the self-adaptive mechanism implemented in our novel homeostatic neuron. The spike signals coming from the PRE neurons are integrated using an Arduino 2 microcontroller, eventually enabling the fire activity when the threshold of the neuron is hit. This causes (i) the 'Out' response of the neuron and (ii) the crystallization signal for the gradual increase of the PCM conductance. In this way the internal threshold V_{TH} of the neuron increases.

network level. In the neuron, the gradual crystallization of a PCM device allows to tune the internal threshold, thus enabling the unsupervised learning of asynchronous multi-density patterns. The learning activity is carried out by self-regulation of the firing activity via PCM devices as a function of pattern specialization. We finally describe the use of PCM devices for detecting correlated signals during the learning activity. These procedures enable fast and stable learning of complex patterns and highlight the fundamental role of bio-inspired computing for artificial intelligence.

II. PCM-BASED NEURONS WITH SELF-ADAPTIVE THRESHOLD

Fig. 1a shows a schematic illustration of spike-frequency adaptation in a neuron cell. When an incoming stimulation excites a neuron, the output firing rate tends to increase, which is counteracted by an adaptation of the internal threshold of the neuron, serving as a negative feedback [25]. In synaptic learning processes, this threshold regulation aims at preventing an unlimited growth of the synaptic conductance weights. As a result, the frequency adaptation balances the learning activity, thus enabling an overall homeostatic mechanism and a consequent better accuracy and stability of classification.

The homeostatic adaptation of Fig. 1a has been applied to a case of the simple winner-take-all (WTA) network shown in Fig 1b. Here, 10 output neurons (POSTs) compete for specializing on 10 input patterns via STDP protocol. Classification is achieved using both excitatory synapses, which allows specialization of the 'winner' neuron to a given pattern, and inhibitory synapses, which instead prevent other neurons to specialize to the same pattern [24]. Each POST is designed as an integrate and fire (I&F) neuron (Fig. 1c), where the threshold potential for fire is regulated by an adaptive threshold block. Synaptic excitatory dynamics are reproduced via STDP protocol using PCM devices switching from low resistive state (LRS) to high resistive state (HRS), and vice versa [26]. Potentiation is achieved when the POST fires after the pre-neurons (PREs), while depression is

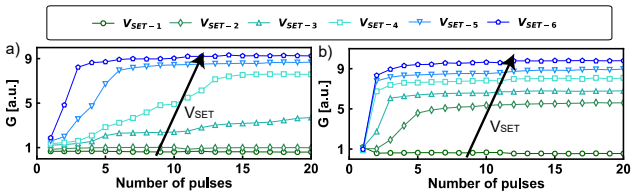

Fig. 3. Experimental measurements of gradual crystallization of the homeostatic PCM device implemented in each neuron.at increasing V_{SET} amplitude for pulse widths t_P = 100 ns (a) and t_P = 200 ns (b).

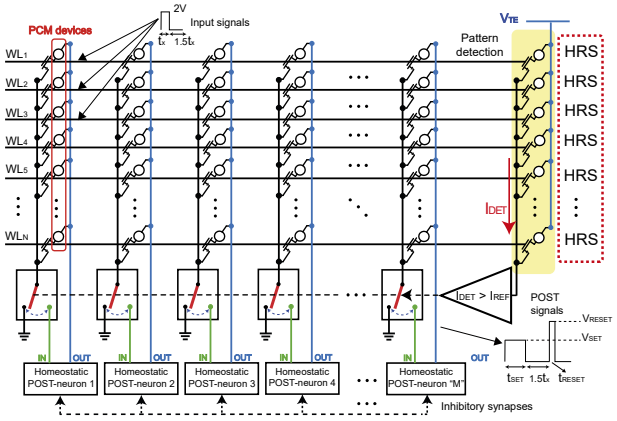

Fig. 4. Implemented setup for asynchronous STDP. Every column connects the WLs, to which inputs are submitted, to a specific POST by 1T1R PCM synapses. A further column of HRS devices is used for pattern/noise detection. The integration activity of each neuron is enabled only for I_{DET}>I_{REF}. Inhibitory synapses are implemented to allow the use as WTA network. The reference time is t_x = 1 ms.

achieved when the POST fires before the PRE [26]. The inhibitory synapses are designed to discharge the POST integrator when a fire of another POST occurs, thus implementing the WTA learning.

A. Hardware realization of the homeostatic neuron

Fig. 2 shows the adaptive threshold circuit, where the spiking frequency is modulated by a reference PCM. PCM devices typically display a relatively large range of analog conductance states [24] where the repeated application of pulses to the top electrode causes the gradual increase of conductance [27, 28]. In the circuit, this feature causes a gradual variation of the threshold voltage.

The circuit works as follows: incoming spikes from PREs induce a synaptic current that is integrated in the "integration" block, experimentally consisting of an Arduino 2 microcontroller. When the voltage reaches the internal threshold V_{TH}, the pulse generator applies three signals: (i) signal 'out' being applied to the next layer of neurons, (ii) a feedback signal applied to synapses for the STDP protocol, and (iii) a crystallization signal applied to the internal PCM device to induce the self-threshold regulation. Each crystallization pulse leads to an incremental set transition of the PCM device to higher conductance G_{PCM}. The PCM conductance controls the fire threshold V_{TH} which is obtained as the read current of the PCM biased at $V_{read} < 0$ after conversion into a transimpedance amplifier, namely $V_{th} = -R_L G_{PCM} V_{read}$, where R_L is the feedback resistance of the transimpedance amplifier in Fig. 2. Initially, since the device is in a high resistive state, I_C and V_{TH} are both low. As the

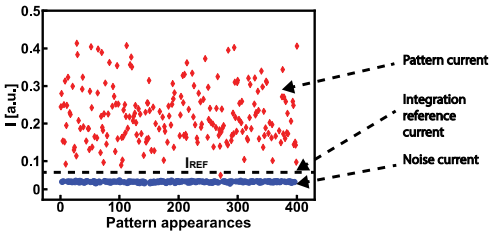

Fig. 5. Measured I_{DET} for 400 Fashion-MNIST images and noise. Only patterns show $I_{DET} > I_{REF}$ while noise has always $I_{DET} < I_{REF}$.

POST fires, the incremental crystallization of the PCM results in a higher threshold. The crystallization event is iterated at every POST fire, causing a continue increase of V_{TH}. As a result of the increasing V_{th}, the fire of the neuron is retarded, namely, the time required by the incoming integrated current to hit the threshold increases. Thus, the spiking frequency of the POST decreases at increasing crystallization of the reference PCM.

Fig. 3 shows the measured PCM conductance G_{PCM} under applied programming pulses at increasing voltage V_{SET} amplitudes for pulse widths t_P = 100 ns (a) and t_P = 200 ns (b). The PCM shows a gradual increase of conductance which suitably reproduces the adaptive threshold regulation of V_{TH}. Note that the crystallization depends on both the amplitude and duration of the voltage pulses. In general, G_{PCM} is more controllably modulated at shorter pulses and intermediate set voltages, with a range of one order of magnitude of achievable intermediate states. The large resistive window can strongly affect the firing rate of the neuron, thus enabling an efficient homeostatic scaling.

III. Unsupervised Learning via STDP

To support the essential role of spike-frequency adaptation in improving learning and energy efficiency, we developed a SNN capable of unsupervised learning by STDP. Patterns are submitted partially and asynchronously, i.e. only parts of them appear at the same moment, with varying density and appearance rate. Fig. 4 shows the designed SNN, where PCM synapses have 1-transistor/1-resistor (1T1R) structure with transistor gates connected by wordlines (WLs) and PCM top electrodes connected by bitlines (BLs). The input signal consists of an alternation of the asynchronous pattern and random noise spikes, where noise, used for background depression, has lower density and frequency [21]. Note that noise can fall in both pattern and background channels. Input spikes are applied to the WLs, in order to induce synaptic currents that are summed at each column to feed the I&F POSTs with self-adaptive threshold, according to the scheme of Fig. 2. An extra column of PCM synapses in HRS is used to discriminate between pattern and noise by monitoring the corresponding current I_{DET}. Fig. 5 shows the measured I_{DET} in response to 400 submissions of 28x28 images from the Fashion-MNIST dataset [29] combined with noise. Data indicate that the submission of a pattern can be detected for $I_{DET} > I_{REF}$. On the other hand, noise always results in a current below the threshold even if it appears at pattern channels, thanks to the smaller density of input spikes. Pattern detection allows to activate the POST integration only for the case of a submitted pattern. Thus,

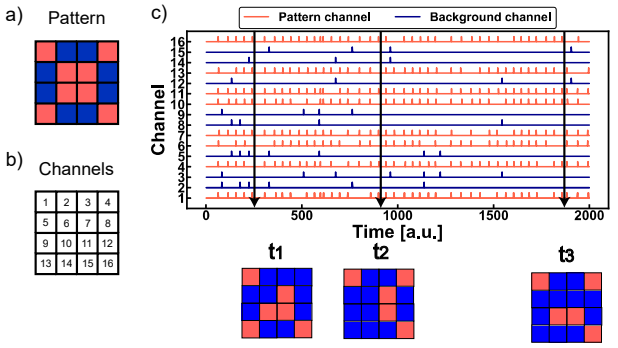

Fig. 6. (a) Experimental measurements of a simple 4x4 pattern. (b) Positions of the 16 channels in relation to pattern and background. (c) The pattern and noise input signals are asynchronously submitted to 16 WLs at high and low frequency, respectively. As a result, the pattern is not always fully presented at the input of the network, as visible in the three snapshots of the signal plot at t_1 t_2 and t_3.

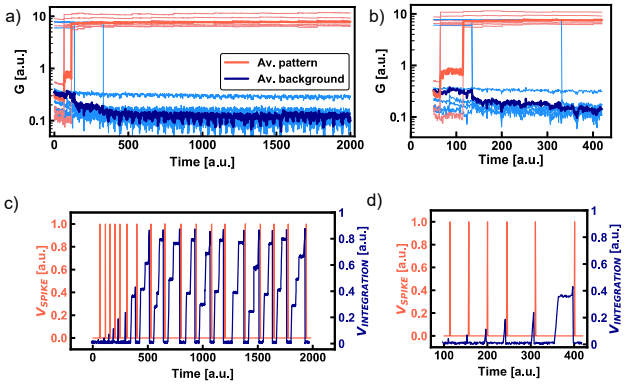

Fig. 7. (a) Experimental measurements of the synaptic evolution of pattern and background synapses during the experiment via asynchronous STDP. (b) Magnification of the first 400 [a.u.] to show the gradual set of the pattern synapses due to asynchronous pattern presentation. (c) Inegration (blue) and fire (red) signals of the POST during the learning activity. The fire rate decreases at increasing time due to the PCM-homeostatic effect of the neuron, while the integration must increase accordingly. (d) Magnification of the first 400 [a.u.].

erroneous noise-induced potentiation effects are prevented even for asynchronous inputs.

A. Experimental results for unsupervised learning

Unsupervised learning by asynchronous STDP, or ASTDP, was tested in our SNN for the asynchronous submission of patterns. Fig. 6 summarizes a simple ASTDP experiment to learn a 4x4 pattern (a) submitted to 16 synaptic channels (b). Fig. 6(c) shows the signals for asynchronous spikes of pattern at relatively high frequency and noise at relatively low frequency. Due to the asynchronous spiking, the pattern is not fully presented at the PRE channels, as illustrated by the snapshots at increasing time t_1, t_2 and t_3. Nevertheless, pattern learning is possible thanks to proper screening of the noise and homeostatic regulation in the POST. This is demonstrated in Fig. 7(a), showing the measured weights of the 16 PCM synapses within the pattern and outside of the pattern, i.e., in background positions. Note that the potentiation is gradual due to the asynchronous signals, Fig. 7(b). As the internal potential reaches V_{th}, the POST fires, causing (i) the synaptic potentiation by STDP and (ii) the increase of the homeostatic PCM conductance, hence V_{th}. Figs. 7(c) and 7(d) show the occurrence of output spikes and the time evolution of V_{th} for the homeostatic regulation. Due

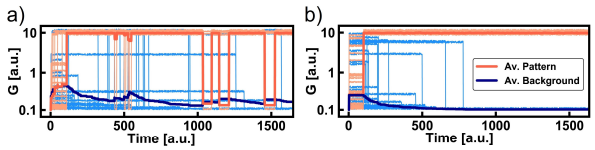

Fig. 8. Synaptic evolutions for a "sandal" pattern from Fashion-MNIST dataset without (a) and with (b) PCM homeostatic control. Only (b) shows fast and stable learning. The bold lines indicate the average evolutions.

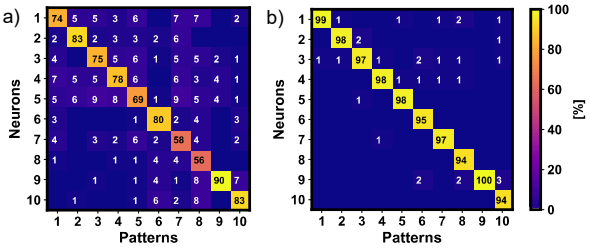

Fig. 9. Confusion matrices for the averaged learning activities of the ASTDP WTA network for the 10 classes of the Fashion-MNIST training dataset without (a) and with (b) homeostasis. Note that the learning accuracy is high and stable only when homeostatic neurons are used in the network, reaching an average learning accuracy of 97%.

to the increase of V_{th}, the POST firing activity decreases, which ensures an improved energy efficiency of the SNN. Note that the integration is disabled during the fire of the POST, in order to avoid the integration of set/reset pulses.

B. Unsupervised learning of multiple patterns

PCM-based homeostasis enables multiple pattern learning by unsupervised ASTDP. In fact, homeostasis allows each POST to adjust its internal V_{th} to the specific pattern for which the POST is specializing. As a result, a POST hardly fires in response to a pattern with similar density, rather it tends to respond only when a specific pattern is presented at the input. This mechanism, in addition to the noise control capability and the WTA design of the network, ensures robust and stable learning.

To test the effectiveness of homeostatic scaling in the WTA approach, we tested our SNN for the classification of 10 images from the Fashion-MNIST dataset. Fig. 8 shows the synaptic weights evolutions of an image of a sandal from the dataset with and without homeostatic mechanism. Learning is unstable without homeostasis (Fig. 8b) as the submission of patterns with a comparable density to the learnt pattern causes unwanted POST fires. Homeostasis, by contrast, leads to an overall optimized behavior of the whole system in terms of learning capability and stability (Fig. 8c). The benefit introduced by the PCM-based homeostasis is clear from Fig. 9, showing the confusion matrices for the learning accuracies of submitted patterns without (a) and with (b) homeostasis. The study is carried out by performing Monte Carlo simulations of the learning activities for the 10 classes of the training dataset with 60000 images. Homeostatic scaling allows for an accuracy increase by about 20% on average, thus highlighting the relevance of PCM-adaptive threshold in WTA SNNs for unsupervised learning.

IV. Robustness of PCM-based Homeostatic Scaling

The self-regulating capability of the neuronal threshold via PCM gradual crystallization, plays a key role to enable

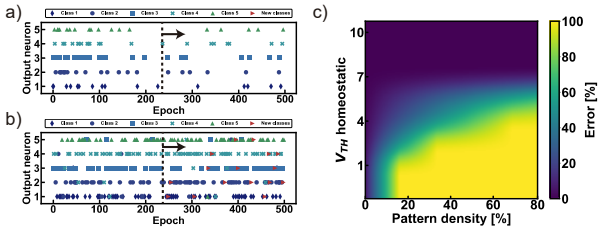

Fig. 10. Fire activities of 5 homeostatic (a) and non-homeostatic (b) neurons in 500 epochs of pattern and noise presentations. The homeostatic neurons show stability even when "false" patterns from another dataset, e.g. MNIST, are shown (after the 250th epoch). (c) Contour plot for the robustness of the POST as a function of the homeostatic PCM conductance and the false pattern density.

homeostatic regulation, resulting in the optimization of WTA networks based on STDP. Furthermore, it introduces robustness in classification when an external perturbation, e.g. a false pattern from another dataset, appears at the input. Fig. 10 shows the comparison between a classification of five images from Fashion-MNIST with (a) and without (b) PCM-based homeostatic neurons. In the first half of the epochs, five images from Fashion-MNIST dataset are presented and classified with no errors for homeostatic neurons, while some errors due to instability are evident in non-homeostatic neurons. In the second half of the epochs, new patterns from the MNIST dataset, consisting of handwritten digits, are presented among the previous ones. The homeostatic neurons do not make errors, while the non-homeostatic ones present further spurious spikes due to the presentations of the false patterns. Fig.10(c) shows the false fire probability as a function of the adaptive threshold. Note that the robustness against spurious fires of various pattern densities is better at relatively high thresholds. These results highlight the homeostatic role of self-adaptive threshold for both specialization in classification accuracy and robustness against external perturbations.

V. Conclusions

This work presents a novel neuron capable of self-regulating its internal threshold relying on the gradual crystallization of PCM devices. The homeostatic neurons are compact, energy-efficient and allow great accuracy and stability in classification tasks using a PCM-based network capable of unsupervised learning via STDP. Furthermore, we demonstrate that the PCM-based homeostatic mechanism gives robustness to the neuromorphic circuit when external perturbations occur. Thus, PCM devices enable bio-inspired local edge computing, and appear to be promising synaptic devices to boost artificial intelligence capabilities.

References

[1] A. Krizhevsky, I. Sutskever, and G.E. Hinton, "ImageNet Classification with Deep Convolutional Neural Networks," International Conference on Neural Information Processing Systems, Proceedings, 2012.

[2] T. Mikolov, A. Deoras, D. Povey, L., Burget, and J. Cernocky, "Strategies for training large scale neural network language models," IEEE Workshop on Automatic Speech Recognition and Understanding, ASRU 2011, Proceedings, 2011.

[3] R. Collobert, J. Weston, L. Bottou, M. Karlen, K. Kavukcuoglu, and P. Kuksa, "Natural language procressing (almost) from Scratch," Journal of Machine Learning Research, vol 12, pp 2493-2537, November 2011.

[4] D. Silver e*t Al.*, "Mastering the game of Go with deep neural networks and tree search," Nature, vol. 529, pp. 484-489, Jan. 2016.

[5] Y. LeCun, Y. Bengio, and G. Hinton "Deep Learning," Nature, vol. 521, pp. 436-444, May 2015.

[6] G. I. Parisi, R. Kemker, J. L. Part, C. Kanan, and S. Wermter, "Continual lifelong learning with neural networks: A review," Neural Networks, 2019.

[7] D. O. Hebb, "The organization of behavior, a neuropsychological theory," Hohn Wiley and Sons, 1949.

[8] G S. Stent, "A physiological mechanism for Hebb's postulate of learning. "Proceedings of the National Academy of Sciences of the United States of America," vol. 70,4 (1973): 997-1001, 1973.

[9] G. G. Turrigiano, "Homeostatic plasticity in neural networks: the more things change, they more they stay the same," Trends in Neuroscience, vol 22, Issue 5, pp 221-227, May 1999.

[10] K. Fox, and M. Stryker, "Integrating Hebbian and homeostatic plasticity: introduction," Philosophical transactions of the Royal Society of London. Series B, Biological Sciences, 372 (1715), 20160413, 2017.

[11] J. Lisman, "Glutamatergic synapses are structurally and biochemically complex because of multiple plasticity processes: long-term potentiation, long-term depression, short-term potentiation and scaling," Philosophical transactions of the Royal Society of London, Series B, Biological sciences, vol. 372,1715 (2017): 20160260, 2017.

[12] T. Masquelier, and S. J. Thorpe, "Unsupervised learning of visual features through Spike Timing Dependent Plasticity," PLOS Computational Biology, vol 3, Issue 2, pp 247-257, February 2007.

[13] K. D. Miller, and D. J. C. Mackay, "The role of constraints in Hebbian Learning," Neural Computation, vol 6, Issue 1, pp 100-126, January 1994.

[14] G. G. Turrigiano, "The Self-Tuning neuron: synaptic scaling of Excitatory synapses," Cell, vol 135, Issue 3, pp 422-435, March 2008.

[15] F. Zenke, B. Poole, S. Ganguli, "Continual learning through synaptic intelligence," International Conference on Machine Learning, pp. 3987-3995, July 2017.

[16] W. C. Abraham and A. Robins, "Memory retention–the synaptic stability versus plasticity dilemma," Trends in neurosciences, vol. 28, 2, pp. 73-78, February 2005.

[17] E. Chicca, F. Stefanini, C. Bartolozzi, and G. Indiveri, "Neuromorphic electronic circuits for building autonomous cognitive systems," Proceedings of the IEEE, vol 102 (9), pp 1367-1388, September 2014.

[18] C. Bartolozzi, and G. Indiveri, "Silicon synaptic homeostasis," Brain inspired cognitive systems, BICS 2006, January 2006.

[19] N. Qiao, C. Bartolozzi, and G. Indiveri, "An ultralow leakage synaptic scaling homeostatic plasticity circuit with configurable time scales up to 100 ks," IEEE transactions on biomedical circuits and systems, vol. 11, 6, pp. 1271-1277, November 2017.

[20] M. Suri, O. Bichler, D. Querlioz, B. Traore, O. Cueto, L. Perniola, V. Sousa, D. Vuillaume, D. Gamrat, B. DeSalvo, "Physical aspects of low power synapses based on phase change memory devices," Journal of applied physics, vol. 112 (5), p 10, September 2012.

[21] G. Pedretti, S. Bianchi, V. Milo, A. Calderoni, N. Ramaswamy and D. Ielmini "Modeling-based design of brain-inspired spiking neural networks with RRAM learning synapses," IEEE International Electron Devices Meeting (IEDM), pp. 28.1. 1-28.1. 4, 2017.

[22] D. Kuzum, S. Yu, and H-S P. Wong, "Synaptic electronics: materials, devices and applications," Nanotechnology, vol. 24, 38, pp. 382001, September 2013.

[23] S. Bianchi, I. Muñoz-Martín, G. Pedretti, O. Melnic, S. Ambrogio, and D. Ielmini, "Energy-efficient continual learning in hybrid supervised-unsupervised neural networks with PCM synapses," 2019 Symposium on VLSI Technology, Kyoto, Japan, pp. 1-2, 2019.

[24] I. Muñoz-Martín, S. Bianchi, G. Pedretti, O. Melnic, S. Ambrogio, and D. Ielmini, "Unsupervised learning to overcome catastrophic forgetting in neural networks," IEEE Journal on Exploratory Solid-State Computational Devices and Circuits, vol. 5 (1), pp 58-66, 2019.

[25] G. Indiveri, B. Linares-Barranco, T. J. Hamilton, A. V. Schaik, R. Etienne-Cummings, T. Delbruck, S. Liu, P. Dudek, P. Häfliger, S. Renaud, J. Schemmel, G. Cauwenberghs, J. Arthur, K. Hynna, F. Folowosele, S. Saighi, T. Serrano-Gotarredona, J. Wijekoon, Y. Wang, K. Boahen., "Neuromorphic silicon neuron circuits," Frontiers in Neuroscience, vol. 5, 2011.

[26] S. Ambrogio, N. Ciocchini, M. Laudato, V. Milo, A. Pirovano, P. Fantini and D. Ielmini, "Unsupervised learning by spike timing dependent plasticity in phase change memory (PCM) synapses," Front. Neurosci. 10:56 (2016), 2016

[27] C. D. Wright, P. Hosseini and J. A. Vazquez Diosdado, "Beyond von-Neumann computing with nanoscale phase-change memory devices," Adv. Funct. Mater. 23, 2248–2254, 2013.

[28] T. Tuma, A. Pantazi, M. Le Gallo, A. Sebastian and E. Eleftheriou, "Stochastic phase-change neurons," Nat. Nanotech., vol. 11, pp. 693–699, 2016.

[29] H. Xiao, K. Rasul and R. Vollgraf, "Fashion-mnist: a novel image dataset for benchmarking machine learning algorithms," arXiv preprint arXiv:1708.07747, 2017.